POTENTIAL OF HYPERSPECTRAL INDICES FOR ESTIMATING CROP RESIDUE COVER

Abderrazak BANNARI [1], Martin CHEVRIER [1], Karl STAENZ [2] and Heather McNAIRN [3]

[1] *Remote Sensing and Geomatics of Environment Laboratory, Department of Geography, University of Ottawa, Ottawa (Ontario), Canada K1N 6N5.*
Tel. (613) 562-5800, Ext. 1042 ; Fax (613) 562-5145; Email: abannari@uottawa.ca
[2] *Alberta Terrestrial Imaging Centre (ATIC), University of Lethbridge, 401, 817 4th Avenue South, Lethbridge, Alberta, Canada T1J 0P3.*
Telephone: (403) 317-9188, Ext. 23; Telecopier: (403) 381-2804; E-mail: karl.staenz@imagingcenter.ca
[3] *Agriculture and Agri-Food Canada, 960, Carling Avenue, Ottawa (Ontario), K1A 0C6*
Telephone: (613) 759-1815; Telecopier: (613) 759-1924; E-mail: mcnairnh@agr.gc.ca

Submitted: February 22, 2007 ; revised: May 17, 2007; accepted September 21, 2007- © *Revue Télédétection*, 2007, vol. 7, n° 1-2-3-4, p. 447-463

Abstract

This study focuses on the potential of hyperspectral indices for estimating crop residue cover in an agricultural environment. Several crop residue indices were compared (BI, CAI, NDI, SACRI, MSACRI and CRIM) in order to identify the ones that are most suitable for crop residue cover estimation. For this purpose, two different and independent data sources were used: ground-based reflectance measurements and hyperspectral Probe-1 data. The spectroradiometric ground-measurements were collected with a GER 3700 spectroradiometer over corn residues at various coverage rates (0 %, 25 %, 40 %, 50 %, 75 % and 100 %). They were convolved and resampled to the Probe-1 spectral band characteristics, and then crop residues were calculated. Moreover, the hyperspectral Probe-1 image was spectrally and radiometrically calibrated, atmospherically corrected, as well as geometrically rectified, after which crop indices were derived. The accuracy of these indices was examined using ground truth obtained from vertical photographs. Compared to ground truth, results indicate that for the ground-based reflectance the best indices for crop residue cover estimation are the CRIM and MSACRI-1 indices with an absolute error estimation of 20 % and 23 %, respectively. For the hyperspectral Probe-1 data, results show that the MSACRI-1 was relatively representative of the ground reference information and outperformed the other indices

Key words : hyperspectral remote sensing, Probe-1 sensor, spectroradiometric measurements, GER 3700, hyperspectral indices, crop residue mapping.

POTENTIEL DES INDICES HYPERSPECTRAUX POUR L'ESTIMATION DU TAUX DE COUVERTURE DES RÉSIDUS DE CULTURES

Résumé

La végétation sèche et les résidus de cultures jouent un rôle important dans la protection de la surface des sols agricoles contre l'érosion hydrique et éolienne. Leur conservation sur les terres agricoles après la moisson a été considérée comme une pratique anti-érosive efficace. Entre autres, ils améliorent non seulement la structure du sol mais également la fertilité de ce dernier par l'addition de nutriments ainsi que par l'addition de matière organique. En plus d'influencer l'infiltration de l'eau dans le sol, l'évaporation, la porosité et la température du sol, les résidus de cultures peuvent également améliorer la qualité de l'eau et ils réduisent les émissions de dioxyde de carbone dans l'atmosphère en le fixant dans le sol. Cette recherche porte sur la comparaison du potentiel de différents indices hyperspectraux (BI, CAI, NDI, SACRI, MSACRI et CRIM) pour l'estimation du taux de couverture des résidus de cultures sur les terres agricoles en exploitant deux sources différentes et indépendantes de données : des mesures spectroradiométriques et une image hyperspectrale aéroportée acquise par le capteur Probe-1. Les mesures spectroradiométriques ont été acquises au sol à l'aide d'un appareil GER 3700 au-dessus des résidus de maïs à différents taux de couverture et au-dessus de divers sols nus (0 %, 25 %, 40 %, 50 %, 75 % et 100 %). Ces mesures ont été ré-échantillonnées et soumises à une convolution spectrale selon les réponses des filtres caractérisant les bandes spectrales du capteur du capteur hyperspectral Probe-1, et les indices ont été calculés. Quant à l'image hyperspectrale, elle a été corrigée des effets atmosphériques, étalonnée spectralement et radiométriquement, et rectifiée géométriquement. Ensuite, les indices ont été dérivés. La précision des indices calculés à partir des mesures au sol et

de l'image hyperspectrale aéroportée a été examinée par rapport à la réalité de terrain obtenue à l'aide des photographies verticales acquises au sol au-dessus de certains points de validation. Par comparaison avec cette réalité de terrain, les résultats obtenus à partir des mesures spectroradiométriques au sol montrent que les indices CRIM et MSACRI-1 performent mieux en estimant le taux de couverture des résidus avec des erreurs absolues, respectivement, de 20 % et 23 %. Quant aux résultats obtenus à partir de l'image hyperspectrale Probe-1, le MSACRI-1 se montre relativement plus adéquat que les autres indices pour l'estimation et la cartographie des résidus de cultures.

Mots-clés : télédétection hyperspectrale, capteur Probe-1, mesures spectroradiométriques, GER 3700, indices hyperspectraux des résidus, résidus de cultures, cartographie.

1. INTRODUCTION

Conservation of crop residues after harvesting is an effective anti-erosive measure (Freebairn and Worcker, 1986). With as little as 15 % corn residue cover, erosion can be reduced by 75 % (Ketcheson and Stonehouse, 1983). As to the environmental aspect, crop residues improve soil structure, increase organic matter content in the soil, and have positive influences on water infiltration, evaporation and on soil temperature (Aase and Tanaka, 1991). They can also play an important role on fixing the carbon dioxide (CO_2) in the soil (Rice, 2002). Adoption of appropriate conservation and restoration practices can build up soil organic carbon by preserving the input of carbon through crop residue and by decreasing carbon loss from soil erosion (Daughtry *et al.,* 2006). Furthermore, data on crop residue cover percentage are useful for input into soil erosion models such as the Universal Soil Loss Equation (Wischmeier and Smith, 1978).

There are several procedures for mapping crop residues in the literature, namely visual estimation (McNairn and Protz, 1993), line transect (Morrison *et al.*, 1993, 1995), point intercept (Daughtry *et al.*, 1995), meter stick (Hartwig and Laflen, 1978), spiked wheel (Morrison *et al.*, 1993), and photographic techniques (Morrison and Chichester, 1991). However, these methods are time consuming, not suitable for large area coverage and very costly to operate over large areas (Daughtry *et al.*, 1996). One challenge of remote sensing, as a potential alternative tool/method for detecting crop residues and for monitoring agricultural fields, is to differentiate residues from bare soil, especially when residues are weathered (Bannari *et al.*, 2000 ; Streck *et al.*, 2002). Over the years, scientists have developed several vegetation indices for the quantitative evaluation of vegetation cover (Bannari *et al.*, 1995a). Due to the absence of chlorophyll in senescent vegetation, these indices are not suitable for crop residue estimation (Bannari *et al.*, 1999 ; Major *et al.*, 1990 ; Cyr *et al.*, 1995). Scientists had to find new spectral ranges more suitable for crop residues (Biard *et al.*, 1995 ; Daughtry, 2001 ; Daughtry *et al.*, 1996, 2004 ; Biard and Baret, 1997 ; Bannari *et al.*, 2000). They developed new indices that are suited for the quantitative evaluation of crop residue cover. Moreover, the development of crop residue indices is difficult because they must be independent of the optical properties of bare soil, colour and brightness (Bannari *et al.*, 1996, 1999). Six major crop residue indices are found in the literature. These are the Brightness Index (BI: Major *et al*., 1990), Cellulose Absorption Index (CAI: Daughtry *et al.*, 1996), Normalized Difference Index (NDI : McNairn and Protz, 1993), Soil Adjusted Corn Residue Index (SACRI: Biard *et al.*, 1995), Modified Soil Adjusted Corn Residue Index (MSACRI: Bannari *et al.*, 2000), and Crop Residue Index Multiband (CRIM: Biard and Baret, 1997). The objective of this study was to determine which index provides the best estimation of crop residue cover using two different and independent sources of data: ground-based reflectance measurements data collected with the GER 3700 spectroradiometer and airborne hyperspectral remote sensing imagery acquired with the Probe-1 sensor.

2. MATERIAL AND METHODS

The objective of this study was to determine which hyperspectral index provides the best estimation of crop residue in agricultural land. The methodology is based on two different and independent sources of data: ground-based reflectance measurements collected with the GER 3700 spectroradiometer and hyperspectral Probe-1 sensor data. For validation purposes, in each case and for each crop residue index, ground truth obtained from multiple vertical photographs was used. A flowchart shown in Figure 1 summarizes the processing steps.

2.1. Study Site

Data were acquired in an agricultural region near Indian Head (50^o 32' N ; 103 ^{o} 40' W), in southern Saskatchewan, located 68 km east of Regina, Canada (Figure 2). The principal economic activities in this area are based on agriculture. Major crops are wheat, pea, canola and corn. The fields (sites) used for validation purposes were located on a precision test farm of the Indian Head Agricultural Research Foundation (IHARF) and geo-referenced using a GPS. This experimental farm was used in the context of a larger project to investigate the potential of hyperspectral remote sensing in precision agriculture. In this project, field measurements, airborne and satellite hyperspectral data were investigated for crop residue mapping (Bannari *et al.*, 2006), plant water content estimation (Champagne *et al.*, 2003), nitrogen stress detection (Karimi *et al.*, 2005a, b), leaf area index (LAI) modelling and percent crop cover types estimation (Pacheco *et al.*, 2001, 2002, 2007), and chlorophyll content prediction (Bannari *et al.*, 2007a).

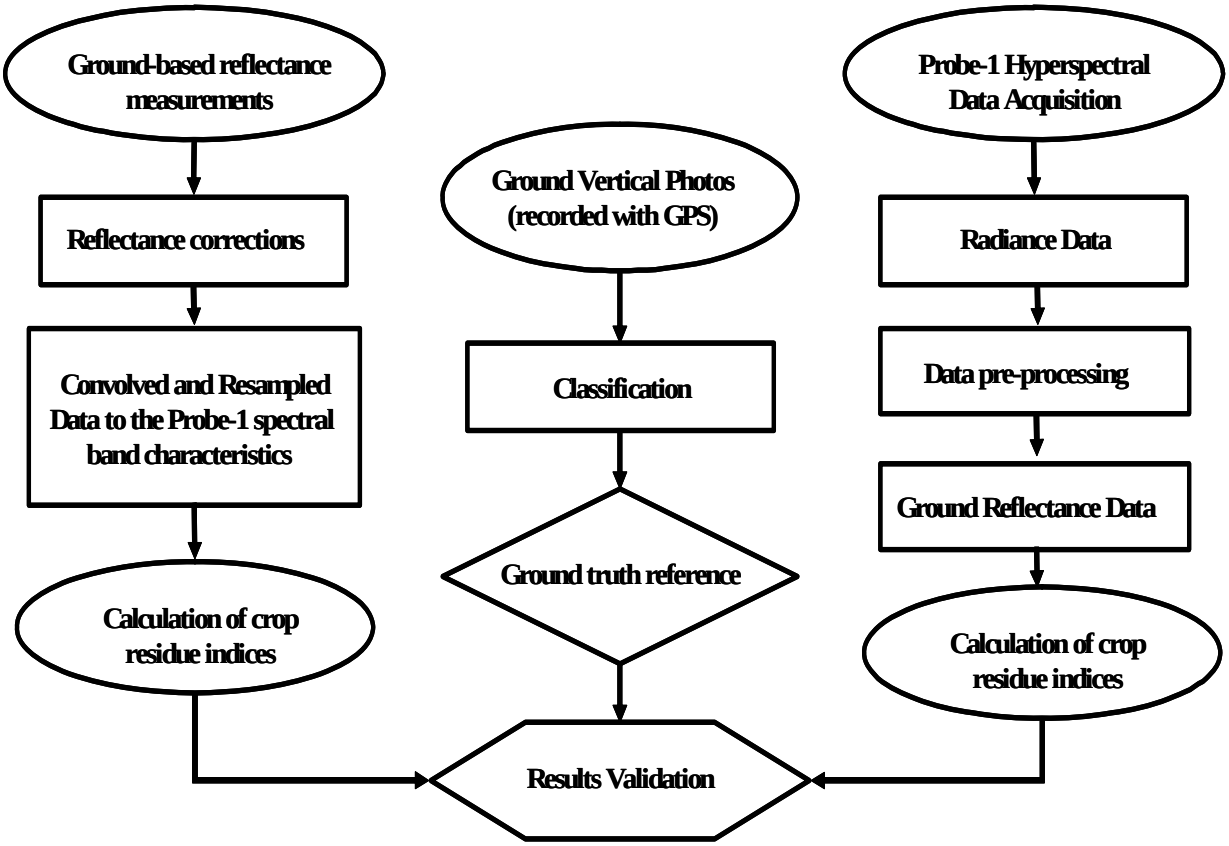


Figure 1 : Processing sequence for crop residue estimation from ground-based reflectance data and from Probe-1 hyperspectral imagery. *Séquence des traitements pour l'estimation des résidus de cultures en utilisant des mesures spectrales au sol et une image hyperspectrale Probe-1.*



Figure 2 : Study site, Indian Head, Saskatchewan. *Site d'étude à Indian Head, Saskatchewan.*

The climate of Indian Head can be regarded as typical northern continental. Hot temperatures and occasional dry periods characterize the summer. The winter is cold and snowy with temperatures remaining below freezing until early

March. The Indian Head area is dominated by Black Chernozemic soils, which developed on neutral to slightly alkaline and uniform clayey lacustrine deposits. Several reasons explain the choice of this study site. First, this site is quite representative of Canadian prairie agricultural lands (Manitoba, Saskatchewan and Alberta). Given that the economy of the Canadian prairies is mainly based on agriculture, it is essential to give a lot of importance to protecting agricultural fields against wind and water erosion. Hence, the importance of crop residue mapping on agricultural fields.

2.2. Hyperspectral Probe-1 data

The data were acquired using the airborne hyperspectral Probe-1 (Earth Search Sciences Inc., 2001) on June 28, 2000 over the Indian Head site (Figure 3). The Probe-1 is a "whiskbroom style" instrument that collects data in the cross-track direction by mechanical scanning and in the along-track direction by movement of the airborne platform. This sensor acquires upwelling radiance in 128 bands in the 400 to 2 500 nm wavelength region. The at-sensor radiance is dispersed by four spectrographs onto four linear detector arrays with 32 bands each. This sensor continuously covers the wavelength range with small gaps in the strong 1 380 and 1 870 nm atmospheric water vapour absorption regions. The bandwidth is between 11 and 18 nm at full width half maximum (FWHM). Probe-1 is mounted on a three-axis gyrostabilizer to minimize geometric distortion from the aircraft movement. The flying altitude was 2 500 m above ground for a swath width of 3 km and a spatial resolution of 5 m by 5 m. A non-differential GPS was recording the location of the aircraft during the flight.

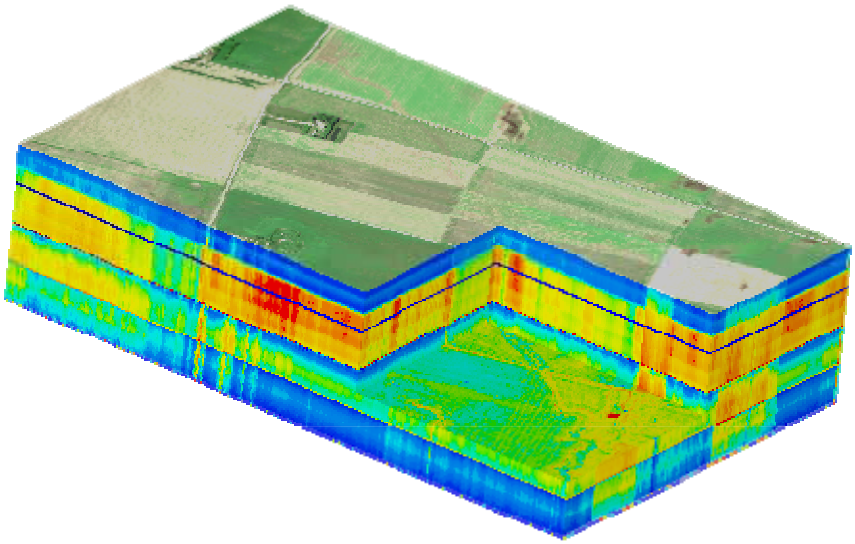


Figure 3 : 3D cube of the Probe-1 hyperspectral image. *Cube en 3D de l'image hyperspectrale Probe-1*.

2.3. Ground data measurements

A series of ground-based reflectance measurements data were collected with the GER 3700 spectroradiometer (Geophysical and Environmental Research Corporation, 1990) from different bare soil samples and different percentages of corn residue ground cover (0 %, 25 %, 40 %, 50 %, 75 % and 100 %). The field-of-view of the GER 3700 was 10° and the distance between the target and the instrument was 1.85 m, which gives a diameter of 32.37 cm on the target. The GER 3700 measures radiance over a spectral range from 400 to 2 500 nm using 704 spectral bands varying from 1.5 nm to ~20 nm at full width half maximum (FWHM). Ground reflectance was calculated by rationing the target radiance with that obtained from a calibrated 25 cm by 25 cm white Spectralon panel (Labsphere, 2001). Corrections were made for wavelength dependence and the non-lambertien behaviour of the panel. The radiance of the Spectralon panel was acquired immediately before the target radiance. For each sample, the average of twenty spectra was convolved with Gaussian response profiles to match the bandwidths and the band centres of the Probe-1 sensor bands. Then crop residues indices were calculated.

For validation purposes, four sites were considered for the airborne hyperspectral data: site 1 is a patch of bare soil only (0 % residue), site 2 is a pure patch of wheat crop residues (100 % residue), site 3 (71 % wheat residue, 9 % bare soil and 20 % vegetation cover) and site 4 (45 % corn residue, 25 % bare soil and 30 % vegetation cover). The sizes of these areas are illustrated in the Figure 4. Considering these sites only for hyperspectral imagery over each validation point, multiple vertical photographs, covering more than one image pixel, were taken with a 35-mm camera equipped with a 28-mm lens. The camera was mounted on an overhead mast and used at a height of 2 m above ground. In this configuration, the camera viewed a ground area of about 5 m^2. These photos were classified using an unsupervised

Isodata classifier in PCI Image Works (PCI Geomatics, 2000) and aggregated into three classes representing crop residue, soil and vegetation (Figure 5). Fractions of each class were converted to percentages of total area. Ground percent of crop residue cover derived from each vertical photo were averaged per site and compared to extracted fractions from the hyperspectral imagery using different indices. Ground validation point locations were referenced in the field using a differential GPS and located on the hyperspectral imagery.

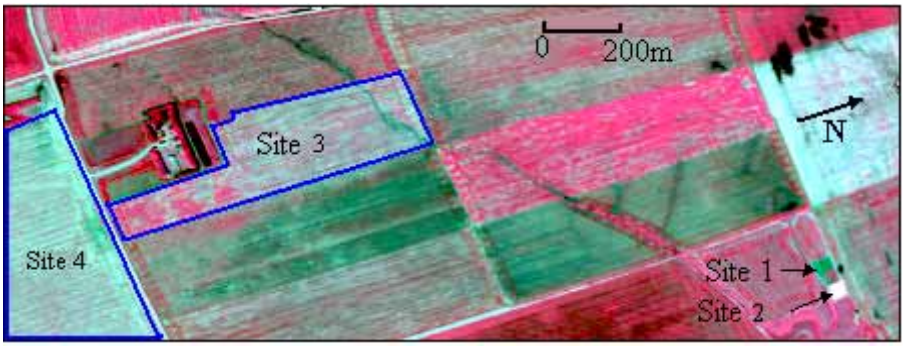


Figure 4 : Location of the validation sites. *Localisation des sites de validation.*

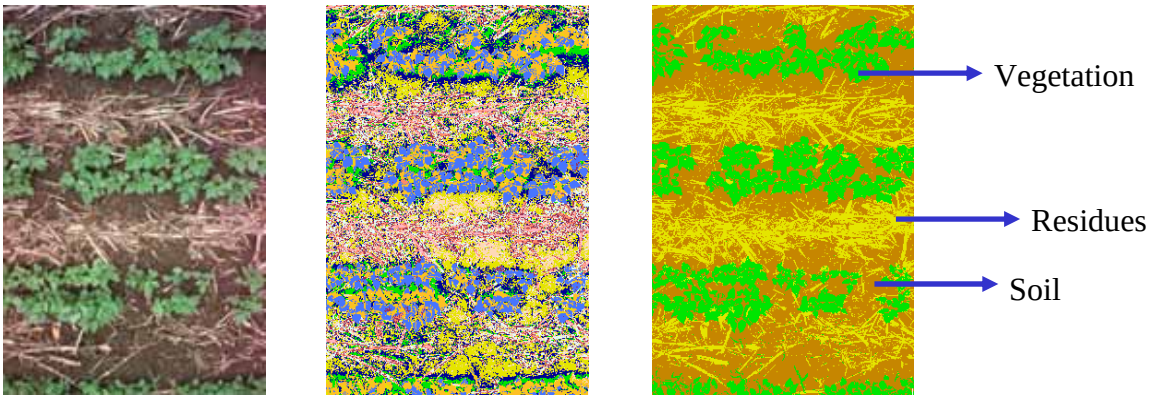


Figure 5 : Classification of ground vertical photographs. *Classification des photographies verticales acquises au sol.*

Moreover, for the validation of the obtained results from ground-based reflectance, after each spectroradiometric measurement a vertical photograph was acquired using the same 35-mm camera. The camera was mounted on the tripod instead of the GER 3700, viewing the same target as the FOV of the spectroradiometer. Then, the photos were classified and the percent crop residue cover calculated as described above. Six different corn residue classes were considered : 0 %, 25 %, 40 %, 50 %, 75 % and 100 %.

Furthermore, for the radiometric sensor calibration, a series of reflectance measurements were collected using the GER 3700 over a pseudo-invariant target (20 m by 30 m asphalt surface). The average of five spectra was convolved with Gaussian response profiles to match the bandwidths and the band centres of the Probe-1 sensor. In order to transform apparent reflectance to ground reflectance, atmospheric parameters were measured with a Microtops-II sun photometer concurrent with the image data acquisition over the study area. From these measurements, the optical depth and water vapour in the atmosphere were extracted.

2.4. Image pre-processing

2.4.1. Radiometric and spectral calibration

Laboratory calibration was completed for the Probe-1 sensor in April 2000 to obtain the dark current signal, radiometric coefficients, and to ascertain the center position of the spectral bands. However, a vicarious calibration of the sensor was required to correct for errors in gains and band centers, which resulted from the stresses experienced during

transportation, installation and operation between the laboratory calibration and the over-flight (Secker *et al.*, 2001). This is an absolute calibration method, which produces a new set of gains that can be used to replace those derived in laboratory. It is also used to correct errors in laboratory spectral calibration since a shift of the band centre positions may have occurred.

To achieve spectral calibration of the Probe-1 data, the raw spectrum (digital numbers) recorded by the sensor was converted to radiance using the radiometric gains and offsets derived in laboratory. The derived reflectance spectra were then analyzed to evaluate the band's center positions using five known atmospheric absorption features located at 760 nm (oxygen), 940 nm and 1 130 nm (water vapour) and 2 005 nm and 2 055 nm (carbon dioxide). Wavelength shifts were then calculated, which best corrected the surface reflectance to obtain a smooth spectrum in the regions of these absorption features. These shifts were then applied to the Probe-1 data. The reflectance-based vicarious calibration was applied to the data using ground-based reflectance measurements of the asphalt target. This site was then visually located in the Probe-1 imagery and an average spectrum extracted. The spectrum from this target was matched to the averaged GER 3700 spectra of the same site. The differences between the two spectra were calculated and the Probe-1 radiometric coefficients were adjusted to minimize the absolute reflectance difference until an error threshold was reached, which was set to 0.02 %. This process is carried out in the *Imaging Spectrometer Data Analysis System* (ISDAS ; Staenz *et al*., 1998) with an iterative numerical technique and provides a new set of optimal gains. These new gains were then applied to the raw digital numbers to calculate at-sensor radiance for the dataset.

2.4.2. Surface reflectance retrieval

The calibrated at-sensor radiance data were converted to surface reflectance using a look-up table (LUT) approach (Staenz and Williams, 1997). Two five-dimensional raw LUTs, and one for a 5 % and 60 % spectrally flat reflectance with tuneable breakpoints were generated with a selected radiative transfer (RT) code to provide additive and multiplicative coefficients for the removal of atmospheric scattering and absorption effects. The MODTRAN-4 RT code (Berk *et al.*, 1999) was applied to the datasets using a Midlatitude Summer atmosphere model and a Continental-Rural aerosol model. The LUTs are then used in combination with a curve-fitting technique in the 940 and 1 130 nm water vapour absorption regions, to estimate the atmospheric water vapour content from the image data themselves on a pixel-by-pixel basis (Green *et al.*, 1991 ; Gao and Goetz, 1990). The column atmospheric water vapour estimates were then interpolated using the LUTs to retrieve surface reflectance.

2.4.3. Image geo-referencing

Airborne imagery generally contains considerable geometric distortion induced by the attitude (pitch, yaw and roll), altitude and speed variations of the aircraft during image acquisition (Bannari *et al.*, 1997). These effects must be eliminated to ensure accurate correspondence between ground measurement locations and image pixel locations. IKONOS imagery was used to establish sampling site locations via an image-to-image registration technique. In the first step, the IKONOS image was geo-referenced using 12 ground control points (GCPs) measured with a differential GPS (± 1 m accuracy). The GCPs were distributed uniformly over the imagery to ensure good image fit (Bannari *et al.*, 1995b). Geo-referencing was done using the WGS-84 geodetic datum to ensure ground-sampling locations were compatible with the image sampling locations. Finally, the ground sampling locations were "burned" in the IKONOS image to ensure that the sampling site positions would remain visible once the geo-referenced image was warped to the Probe-1 imagery. The geo-referenced IKONOS image was then registered to the Probe-1 imagery and warped using a 2^{nd} order polynomial. The average root mean square error (RMSE) of the polynomial fit was 0.7 pixels. The IKONOS image was used as the "slave" image and the Probe-1 imagery was used as the "master" to ensure that the Probe-1 image would maintain radiometric fidelity. A cubic convolution-resampling scheme was applied in the registration procedure, which uses a four-by-four pixel window to compute a ground reflectance as the weighted average of the nearest 16 pixels. Finally, sampling site pixel and corresponding line coordinates from the warped IKONOS were kept for each site and retained for data extraction.

2.5. Crop residue indices

Major *et al.* (1990) developed the BI, which uses the first four bands of Landsat TM. It has been proven that the BI is dependent on the optical properties of bare soil (Bannari *et al.*, 1999). Daughtry *et al.* (1996) based their study on the absorption of cellulose between 1975 nm and 2 225 nm for the discrimination of crop residue and bare soil and came up with the CAI. Although studies have shown that the CAI is independent of the optical properties of bare soil, it has also been demonstrated that it is only suited for small amounts of crop residue cover (Haboudane *et al.*, 1997). McNairn and Protz (1993) reported the sensitivity of the near infrared (NIR) and created the NDI, which is based on the same concept as the NDVI (Rouse *et al.*, 1974) but where red and NIR bands are substituted with NIR and SWIR bands. The NDI is affected by the optical properties of bare soil. However, this index gives good results when using Landsat-7 ETM+ band 5 (ETM-5) and band 7 (ETM-7) (Bannari *et al.*, 1999). In order to minimize the effect of the optical properties of bare soil of the NDI, Biard *et al.* (1995) proposed the SACRI, which integrates the soil line concept. The principles for this index are based on a transformation of the SAVI (*Soil Adjusted Vegetation Index*) (Huete, 1988) to the TSAVI (*Transformed Soil Adjusted Vegetation Index*) (Baret *et al.*, 1989). The SACRI is less sensitive to the optical properties of bare soil than the NDI, and works better with small amounts of crop residue cover (Arsenault and Bonn, 2001).

Another crop residue index was developed by the modification of the SACRI into MSACRI (Bannari *et al.*, 2000). This index uses two specific SWIR spectral bands, ETM-5 and ETM-7. The interest in using these two spectral bands is because this region of the spectrum is recognized as being favourable for identifying various types of rocks, soils, dry vegetation as well as green vegetation. This index gives good results and is independent of the optical properties of bare soil (Bannari *et al.*, 2000). Biard and Baret (1997) developed the CRIM, which uses a linear unmixing model to extract the fraction corresponding to crop residue from the soil-residue complex. Unlike other indices, where specific regions of the spectrum are used, the CRIM may be applied to any set of spectral bands to discriminate crop residue from bare soils. The results with the CRIM are a direct estimation of residue cover fraction in the range of 0 to 1. Research has demonstrated that the CRIM is not sensitive to variations in soil optical properties as a result of changes in moisture and roughness levels (Biard and Baret, 1997). The equations of these indices are as follows:

$$BI = \rho_{TM1} + \rho_{TM2} + \rho_{TM3} + \rho_{TM4} \quad (1)$$

$$CAI = [0.5 * (\rho_x + \rho_y) - \rho_z] \quad (2)$$

$$NDI = (\rho_{TM4} - \rho_{TM5})/(\rho_{TM4} + \rho_{TM5}) \quad (3)$$

$$SACRI = \alpha\,(\rho_{TM4} - \alpha\,\rho_{TM5} - \beta) / (\alpha\,\rho_{TM4} + \rho_{TM5} - \alpha\beta) \quad (4)$$

$$MSCARI = C^{ste}\,[a\,(\rho_{ETM5} - a\,\rho_{ETM7} - b)] / (a\,\rho_{ETM5} + \rho_{ETM7} - ab) \quad (5)$$

$$CRIM = \frac{Cos(\delta)}{Cos(\zeta)} * \sqrt{\frac{1 - \cos^2(\delta)}{1 - \cos^2(\zeta)}} \quad (6)$$

where,

ρ_{TM1} : is the reflectance measured in Landsat TM band 1 (TM-1) ;

ρ_{TM2} : is the reflectance measured in Landsat TM band 2 (TM-2) ;

ρ_{TM3} : is the reflectance measured in Landsat TM band 3 (TM-3) ;

ρ_{TM4} : is the reflectance measured in Landsat TM band 4 (TM-4) ;

ρ_{TM5} : is the reflectance measured in Landsat TM band 5 (TM-5) ;

ρ_{ETM5} : is the reflectance measured in Landsat ETM band 5 (ETM-5) ;

ρ_{ETM7} : is the reflectance measured in Landsat ETM band 7 (ETM-7) ;

ρ_x : is the reflectance measured between 1 975 and 2 025 nm ;

ρ_y : is the reflectance measured between 2 175 and 2 225 nm ;

ρ_z : is the reflectance measured between 2 075 and 2 125 nm ;

α : is the slope of the soil line (TM-4/TM-5) ;

β : is the ordinate at the origin of the soil line (TM-4/TM-5) ;

C^{ste} : is a multiplicative constant of 5 ;

a : is the slope of the soil line (ETM-5/ETM-7) ;

b : is the intercept of the soil line (ETM-5/ETM-7) ;

δ : is the angle between a point (M, residue cover to be estimated) and soil line ;

ζ: is the angle between the soil line and residues line.

Instead of using TM-1 through TM-5, ETM-5 and ETM-7 to calculate these different indices, the reflectance measurements of the GER 3700, convolved and resampled to the Probe-1 hyperspectral bands, are used. The resampled Probe-1 bands with centre wavelengths closest to those of the TM or ETM bands were selected. Therefore, instead of

using TM-1, TM-2, TM-3, TM-4, TM-5, ETM-5 and ETM-7, bands 5 (491 ± 8 nm), 10 (567.5 ± 7.75 nm), 17 (675.7 ± 8.2 nm), 27 (827.6 ± 8.4 nm), 104 (2 109.7 ± 10.05 nm), 84 (1 655.8 ± 7.3 nm) and 110 (2 216.5 ± 9.55 nm) of the Probe-1 hyperspectral sensor were used respectively. Furthermore, the most successful Probe-1 hyperspectral sensor bands for discriminating crop residue from bare soil, those centred at 943 and 2 303 nm (Probe-1 bands 36 (943 ± 7.85 nm) and 115 (2 303 ± 8.95 nm), respectively), were also used to derive the NDI, SACRI and MSACRI indices. These bands are centred. The selection of these two bands was based on the first derivative of corn crop residue and bare soil analysis (with respect to the wavelength), and based on the separability between the soil and crop residue using ground-based spectroradiometric data as well as Probe-1 imagery (Chevrier *et al.*, 2002). The soil line parameters (a and b) were calculated from spectroradiometric measurements using only bare soil (Biard and Baret, 1997 ; Bannari *et al.*, 2000).

3. RESULTS AND DISCUSSION

3.1. Ground Data

Figure 6 provides the results of the BI for corn residue, and shows a dynamic range from 25 % to 81 %. As the residue coverage increases, the BI also tends to increase. When the coverage rate exceeds 75 %, it is shown that there is a saturation problem. Compared to the ground reference measurements (derived percentage of residue cover from the ground vertical photographs), this index tends to overestimate the coverage rate when the residue cover is less than 60 %. When the residue is completely absent and only bare soil is present, this index provides a value of 25 % residue cover. However, the BI underestimates the coverage rate when the corn residue cover exceeds 70 %. The absolute error calculated between ground truth and estimated values from the spectroradiometric ground-measurements were used as an accuracy assessment for the performance of different indices, this measure is 20 % for the BI.

Although studies have shown that the CAI is independent of the optical properties of bare soil and suited for small amounts of crop residue cover in mixed scenes (Nagler *et al.*, 2003 ; Haboudane *et al.*, 1997), this study demonstrates that the CAI is less accurate than the other indices especially for bare soil (0% residues) and sparse corn residue cover. This index describes the average depth of the cellulose absorption feature at the 2.1 mm in reflectance spectra. However, these absorption features are absent in soil and vegetation spectra, and very hard to detect in the pixels with less residue coverage rate. For example, many CAI values were negative and ranged from –104 % to 85 % (Figure 7). The CAI generally underestimated the surface coverage of corn residues and performed poorly at coverage rates lower than 50 %. The index performed better when the residue coverage was greater than 50%. In general, the absolute error of the CAI is 68 %. Bannari *et al.* (1999) and Chevrier (2002) obtained similar results using spectroradiometric ground measurements, and considering different soil types, different residues types (wheat, corn, barley, soya, sunflower), and different residues percentages in an agricultural environment.

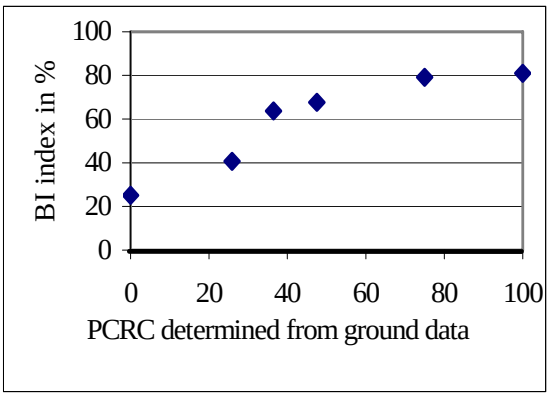


Figure 6 : Relationship between PCRC (percent corn residue cover) obtained with BI from the GER 3700 data resampled to the Probe-1 hyperspectral bands, and ground vertical photographs. *Relation entre le pourcentage du taux de résidus obtenu à l'aide du BI calculé à partir des données GER 3700, rééchantillonné dans les bandes du Probe-1, et celui dérivé des photographies verticales.*

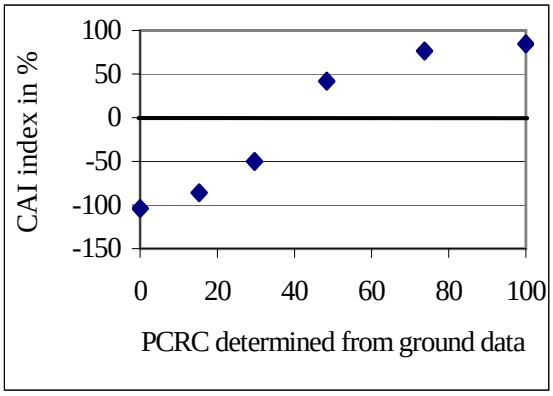


Figure 7 : Relationship between PCRC (percent corn residue cover) obtained with CAI from the GER 3700 resampled to the Probe-1 hyperspectral bands, and ground vertical photographs. *Relation entre le pourcentage du taux de résidus obtenu à l'aide du CAI calculé à partir des données GER 3700, rééchantillonné dans les bandes du Probe-1, et celui dérivé des photographies verticales.*

Two sources of data will be presented for the NDI. NDI-1 is the traditional index, where the reflectance measurements from the GER 3700 were convolved to 827.6 ± 8.4 nm (band 27) and 2 109.7 ± 10.05 nm (band 104) of the Probe-1 sensor. NDI-2 is a modified index, which uses 943 ± 7.85 nm (band 36) and 2 303 ± 8.95 nm (band 115), the most successful bands of the Probe-1 hyperspectral sensor found to discriminate crop residues from bare soil (Chevrier, 2002). Figure 8 illustrates the results obtained and several observations can be made. First, it is evident that the traditional index (NDI-1) is less effective than the modified index (NDI-2). For example, many of the NDI-1 values are negative and they range only from -9 % to 3 %. The traditional NDI-1 index was not able to properly estimate the amount of crop residue. These observations corroborate the Bannari *et al.* (1999) results. On the other hand, NDI-2 values are closer to the measured residue coverage values and ranged from 9 % to 32 %. Both indices tend to underestimate the percentage of corn residue. The absolute errors were 58 % for NDI-1 and 35 % for NDI-2. Furthermore, when the corn residue coverage rate exceeded 75 %, the NDI-2 saturated. In fact, the NDI-2 value slightly decreased when the coverage rate ranged from 75 % to 100 %. In conclusion, it appears that NDI-2 is a better estimator than NDI-1, especially when the residue coverage rate is below 35 %.Using the same spectral bands as in the NDI-1 and NDI-2, two versions of the SACRI index were calculated. Figure 9 illustrates that the traditional index (SACRI-1) is less effective than the modified index (SACRI-2). Negative values were generated with the SACRI-1, the value range was very small and did not reflect the real dynamic range of residue cover in the observed ground data, -1 % to 6 %. In comparison, the values retrieved using the SACRI-2 were relatively higher, 8 % to 42 %. Despite the acceptable performance of the SACRI-2 in estimating coverages lower than 45 %, this index is very sensitive to the soil background. Indeed, Figure 9 shows that for bare soil (0 % crop residue) the SACRI-2 value is approximately 18 %. In addition, it performs poorly at coverages above 60 % and a saturation problem arises when the coverage rate exceeds 75 %. Considering different coverage rates, the absolute errors were very high 55 % and 29 % for SACRI-1 and SACRI-2, respectively.

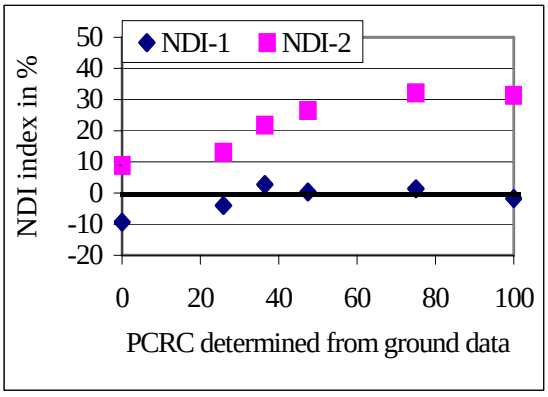


Figure 8 : Relationship between PCRC (percent corn residue cover) obtained with NDI from the GER 3700 resampled to the Probe-1 hyperspectral bands, and ground vertical photographs. *Relation entre le pourcentage du taux de résidus obtenu à l'aide du NDI calculé à partir des données GER 3700, rééchantillonné dans les bandes du Probe-1, et celui dérivé des photographies verticales.*

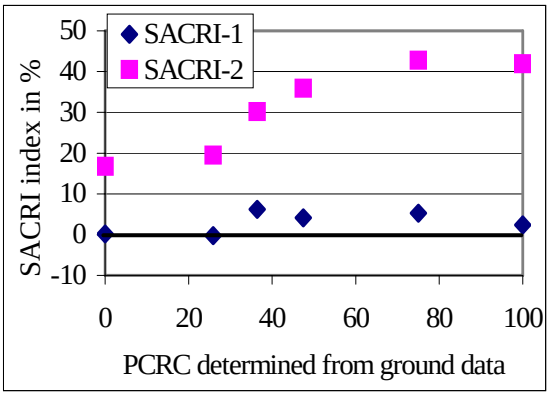


Figure 9 : Relationship between PCRC (percent corn residue cover) obtained with SACRI from the GER3700 resampled to the Probe-1 hyperspectral bands, and ground vertical photographs. *Relation entre le pourcentage du taux de résidus obtenu à l'aide du SACRI calculé à partir des données GER 3700, rééchantillonné dans les bandes du Probe-1, et celui dérivé des photographies verticales.*

Two versions of MSACRI were also tested: the traditional index (MSACRI-1) where reflectance measurements of the GER 3700 were convolved and resampled to 1 655.8 ± 7.3 nm (band 84) and 2 216.5 ± 9.55 nm (band 110) of the Probe-1 sensor, whereas the modified index (MSACRI-2) used 943 ± 7.85 nm (band 36) and 2 303 ± 8.95 nm (band 115). As with the SACRI, the soil-line concept was considered in a 2 dimension spectral space, 1 655.8 nm vs. 2 216.5 nm and 943 nm vs. 2 303 nm were used for MSACRI-1 and MSACRI-2, respectively. Figure 10 shows that MSACRI-1 is more effective than MSACRI-2 for corn residue estimation. In fact, considering different corn residue coverage rates (0 % to 100 %) on the ground, MSACRI-1 estimated the dynamic range in residue cover to be 4 % to 73 % with an absolute error of 23 %. This index is relatively more accurate for sparse rate cover lower than 50 %. In comparison, the values range retrieved from MSACRI-2 varied from 1 % to 133 % with an absolute error of 40 %. As illustrated in Figure 10, MSACRI-2 overestimates the coverage rate and saturates when the coverage rate exceeds 75 %.

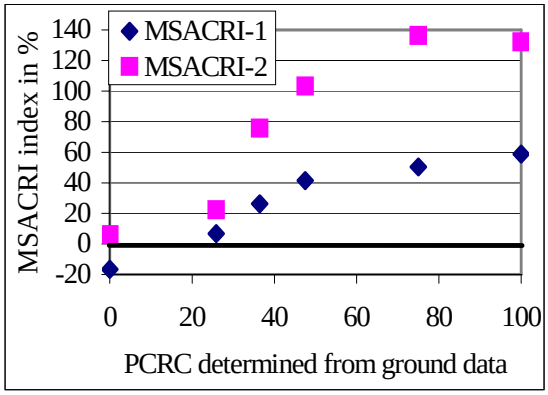


Figure 10 : Relationship between PCRC (percent corn residue cover) obtained with MSACRI from the GER 3700 resampled to the Probe-1 hyperspectral bands, and ground vertical photographs. *Relation entre le pourcentage du taux de résidus obtenu à l'aide du MSACRI calculé à partir des données GER 3700, rééchantillonné dans les bandes du Probe-1, et celui dérivé des photographies verticales.*

To retrieve the soil and crop residue line parameters in the 2 dimension spectral space for the CRIM index, 943 ± 7.85 nm (band 36) and 2 303 ± 8.95 nm (band 115) were used (Chevrier, 2002). The value range of the CRIM index varied from 19 % to 95 % (Figure 11). The CRIM values increased when the ground measured residue coverage increased. However, this index shows very high sensitivity to the soil optical proprieties (only bare soil, 0 % residue) and always overestimates the corn residue coverage, except when residue coverage is 100 %. In this case, the estimated value is 95 %. The average absolute error attached to this index is 20 %. The linearity of the index is not perfect and a saturation problem occurs when the coverage rate exceeds 75 %.

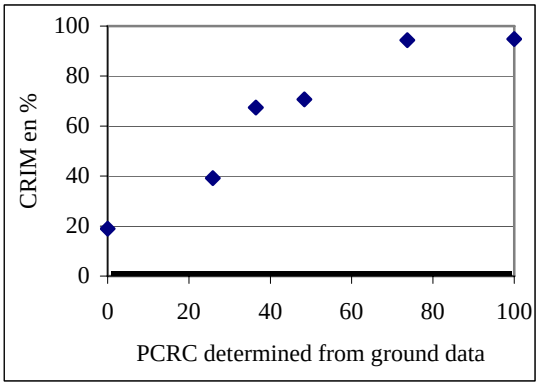


Figure 11 : Relationship between PCRC (percent corn residue cover) obtained with CRIM from the GER 3700 resampled to the Probe-1 hyperspectral bands, and ground vertical photographs. *Relation entre le pourcentage du taux de résidus obtenu à l'aide du CRIM calculé à partir des données GER 3700, rééchantillonné dans les bandes du Probe-1, et celui dérivé des photographies verticales.*

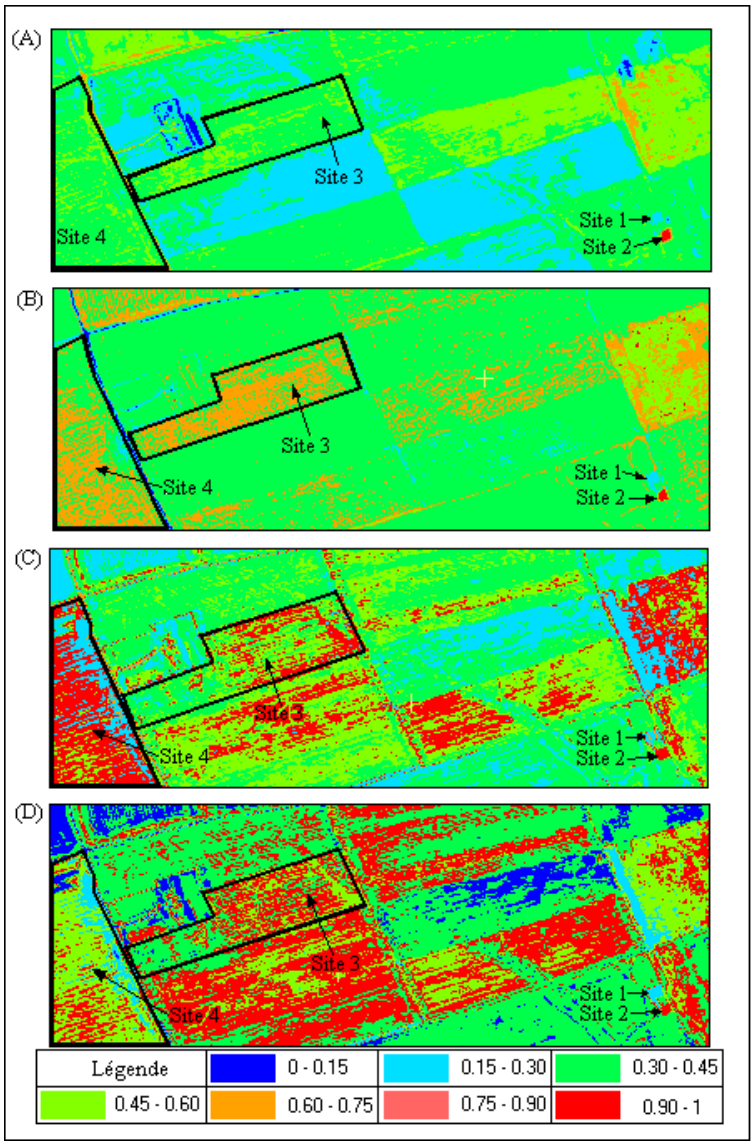


Figure 12 : BI (A), CAI (B), NDI-1 (C), and NDI-2 (D) indices extracted from Probe-1 imagery. *Les indices BI (A), CAI (B), NDI-1 (C) et NDI-2 (D) dérivés de l'image Probe-1.*

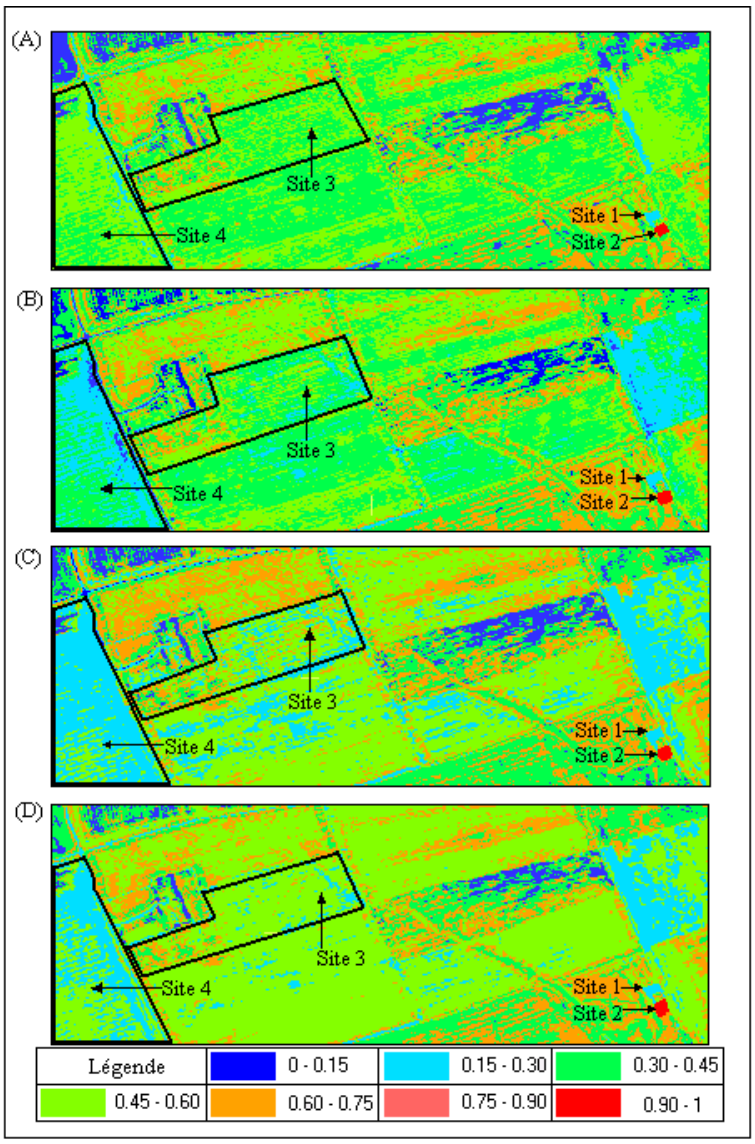


Figure 13 : SACRI-1 (A), SACRI-2 (B), MSACRI-1 (C), and MSACRI-2 (D) indices extracted from Probe-1 imagery. *Les indices SACRI-1 (A), SACRI-2 (B), MSACRI-1 (C) et MSACRI-2 (D) dérivés de l'image Probe-1.*

The performance of the considered indices are summarized and listed according to their absolute error estimation. The index with the smallest absolute error was the BI (20 %), followed by the CRIM (20 %), the MSACRI-1 (23 %), the SACRI-2 (29 %), the NDI-2 (35 %), the MSACRI-2 (40 %), the SACRI-1 (55 %), the NDI-1 (58 %) and the CAI (68 %). Surprisingly, the BI had smaller absolute error estimation than the CRIM, SACRI or MSACRI, which take into account the soil-line concept in their calculation. The soils at the IHARF farm were dark (low reflectance), which obviously benefited the BI. The results would not have been the same if the soils would have been brighter. In fact, due to the BI equation, the estimation of corn residues would have been much higher and the absolute error would have increased (Bannari *et al.*, 1999). Therefore, using GER 3700 ground-based spectroradiometer measurements convolved and resampled to the Probe-1 hyperspectral bands, the CRIM and MSACRI-1 perform better than the other indices considered for estimating the coverage rate of corn residue.

3.2. Image data

The results based on the image data were focused on four validation sites at the IHARF farm (Figure 4). Sites 1 and 2 were patches of pure bare soil and pure wheat residue, respectively. Site 3 had a wheat residue cover of 71 %, bare soil cover of 9 % and vegetation cover of 20 %. Whereas, site 4 had a corn residue cover of 45 %, bare soil cover of 25 %

and vegetation cover of 30 %. Comparative to the ground reference measurements, the crop residue cover estimations on the different validation sites using different hyperspectral crop residue indices are summarized in Tables 1a, 1b, 1c and 1d. In addition, Figures 12 and 13 present the crop residue maps derived from the empirical indices BI, CAI, NDI-1 and NDI-2, and semi-empirical indices SACRI-1, SACRI-2, MSACRI-1 and MSACRI-2. The different values of the indices were grouped into seven classes (Class 1 = 0-0.15 ; Class 2 = 0.15-0.30 ; Class 3 = 0.30-0.45 ; Class 4 = 0.45-0.60 ; Class 5 = 0.60-0.75 ; Class 6 = 0.75-0.90 ; Class 7 = 0.90-1.00).

Table 1a : Estimation of crop residue cover for site 1. *Estimation du taux de couverture des résidus sur le site 1.*

Site 1 (0 % residue cover)	Estimation
BI	15 – 30 %
CAI	15 – 30 %
NDI-1	15 – 30 %
NDI-2	15 – 30 %
SACRI-1	15 – 30 %
SACRI-2	15 – 30 %
MSACRI-1	15 – 30 %
MSACRI-2	15 – 30 %

Table 1b : Estimation of crop residue cover of site 2. *Estimation du taux de couverture des résidus sur le site 2*

Site 2 (100 % residue cover)	Estimation
BI	90 – 100 %
CAI	90 – 100 %
NDI-1	90 – 100 %
NDI-2	90 – 100 %
SACRI-1	90 – 100 %
SACRI-2	90 – 100 %
MSACRI-1	90 – 100 %
MSACRI-2	90 – 100 %

Table 1c : Estimation of crop residue cover of site 3. *Estimation du taux de couverture des résidus sur le site 3*

Site 3 (71.32 % residue cover)	Estimation
BI	30 – 60 %
CAI	60 – 75 %
NDI-1	30 – 60 % and 90 – 100 %
NDI-2	90 – 100 % and 30 – 60 %
SACRI-1	30 – 60 %
SACRI-2	30 – 60 %
MSACRI-1	45 – 75 %
MSACRI-2	45 – 60 %

Table 1d : Estimation of crop residue cover of site 4. *Estimation du taux de couverture des résidus sur le site 4*

Site 4 (44.62 % residue cover)	Estimation
BI	30 – 60 %
CAI	60 – 75 %
NDI-1	90 – 100 %
NDI-2	45 – 60 %
SACRI-1	30 – 60 %
SACRI-2	30 – 45 %
MSACRI-1	45 – 60 %
MSACRI-2	45 – 60 %

With regard to the BI, shown in Figure 12 (A), several conclusions can be drawn. Site 2 (100 % wheat residue cover) was estimated perfectly with a value between 90 % and 100 %. As for site 1 (bare soil, 0 % residue cover), the BI estimated the amount of crop residue to be between 15 and 30 %. As to the ground measurements, the BI is very sensitive to the soil background. For site 3 (71 % wheat residue cover, 9 % bare soil cover and 20 % vegetation cover), the BI underestimated the amount of residue by 30 % to 60 %. In addition, absolutely no pixels representing soil were shown on this site. For site 4 (45 % corn residue cover, 25% bare soil cover and 30 % vegetation cover), the BI provided a good estimation for the residue amount (30 % to 60 %), but once again, the results showed no bare soil. Therefore, the results obtained with the BI were not very accurate in estimating the amount of residue. When the coverage rate is between 40 % and 75 %, the BI underestimated the coverage rate.

The results retrieved with CAI are shown in Figure 12 (B). As for the BI, the CAI correctly estimated the amount of a very dense residue cover from site 2, with values between 90 % and 100 %. This result is approximately similar to the residue estimation from ground measurements. Site 1 (0% residue cover) again had an estimation error between 15 % and 30 % residue cover. Also, the amount of crop residue from site 3 was overestimated. Almost all pixels from site 3 indicate a coverage rate of crop residue between 60 % and 75 %. Again, no pixels representing bare soil were shown. For site 4, the CAI greatly overestimated the amount of residues. Again, most of the pixels estimate the coverage rate between 60 % and 75 %, while the actual coverage rate was 45 % and no bare soil was shown even if the portion of bare soil was 25 %. The results show that the CAI does not accurately estimate the amount of crop residue. In general, compared to the ground truth, the retrieved information from the hyperspectral imagery using the CAI tends to overestimate the residue coverage rate.

The derived information considering the empirical models NDI-1 and NDI-2 are shown in Figures 12 (C) and (D). For both indices, site 2 (100 % wheat residue cover) was correctly estimated with values between 90 % and 100%. With regard to site 1 (bare soil, 0 % residue cover), NDI-1 and NDI-2 estimated the amount of residue with an error between

15 % and 30 %. When observing the results on site 3 (71% wheat residue cover), NDI-1 estimated the residue amount to be between 30 % and 60 %, and NDI-2 between 90 % and 100 %, and no bare soil was shown using these two indices. In fact, for NDI-2 the large majority of pixels overestimated the coverage rate. For NDI-1, one third of the pixels correspond to 30 % – 45 % residue cover, one third to 45 % - 60 % residue cover and one third to 90 % - 100 % residue cover. As for site 4 (45 % corn residue cover), NDI-1 greatly overestimated the amount of residue cover. Most of the pixels were mapped as having a residue cover of 90 % to 100 %. About one tenth of the pixels were mapped as residue cover of 15 % to 30 %, which obviously represents bare soil. The NDI-2 index was a little better than NDI-1 in estimating the amount of residues. The majority of pixels were mapped as residue cover of 45 % to 60 %. However, one third of the pixels were mapped as 90 % to 100 % residue cover and one tenth between 15 % and 30 %, which again represents the bare soil. The results obtained with NDI-1 and NDI-2 are not satisfactory and do not perform accurately enough for crop residue estimation from hyperspectral data.

The results obtained from SACRI-1 and SACRI-2 are shown in Figures 13 (A) and (B). With regard to site 2 (100 % wheat residue cover), both indices perfectly estimated the residue cover between 90 % and 100 %. For site 1 (bare soil, 0 % residue cover), SACRI-1 and SACRI-2 estimated the amount of residue to be between 15 % and 30 %, while for site 3, both indices underestimated the coverage rate. The large majority of the pixels were mapped as residue cover of 30 % to 60 %. No bare soil was shown for both indices. With regard to site 4 (45 % corn residue cover), SACRI-1 estimated the amount of residue to be between 30 % and 60 %, but only a few pixels were classified as bare soil. On the other hand, SACRI-2 accurately estimated the amount of residue from site 4. In fact, half of the pixels were classified as 30 % to 45 % residue cover, with the remaining pixels having a 15 % to 30 % residue cover (bare soil). In conclusion, both indices underestimated the amount of residue on site 3, but SACRI-2 was very accurate in classifying corn residue in site 4.

Figures 13(C) and (D) show the obtained results from MSACRI-1 and MSACRI-2, respectively. By reference to the ground truth, both indices estimated the amount of residue on site 2, 100 % wheat residue, with an absolute difference of 10 %. For site 1 (bare soil, 0% residue cover), the MSACRI-1 and MSACRI-2 estimated the amount of residues to be between 15 % and 30 %. With respect to site 3, MSACRI-1 accurately estimated the amount of residues. In fact, the large majority of the pixels were mapped as residue cover of 45 % to 75 % while some pixels were assigned to 15 % to 30 % residue cover, which represents bare soil (9 %). MSACRI-2 was not as accurate as MSACRI-1. The vast majority of the pixels were mapped as residue cover of 45 % to 60 %. For site 4 (45 % corn residue cover, 25 % bare soil cover and 30 % vegetation cover), the results of MSACRI-1 and MSACRI-2 were very similar. Half the pixels were estimated to have a residue cover between 15 and 30 % while the other half were between 45 % and 60 %. Compared to the results obtained from the imagery, the MSACRI-1 results were relatively accurate for the estimation of the amount of residue.

Finally, according to Biard and Baret (1997), unlike the other indices where specific regions of the spectrum are used, the CRIM may be applied to any set of spectral bands to discriminate crop residue from bare soil, although, it was very difficult or impossible to retrieve the soil and crop residue lines in “N” dimensions, using the 128 Probe-1 bands. Very often, mixed and confused information is obtained that is not helpful in deriving information about crop residue. In addition, we retrieved the CRIM maps using different band combinations, but we never got similar results to what was published (Biard and Baret, 1997) or to ground-based reflectance measurements. Consequently, we do not consider the CRIM performance analysis from the hyperspectral data.

In spite of the relatively acceptable performance of MSACRI-1, several error sources in estimating percent residue cover remain. All the considered crop residue indices have the disadvantage of being less rigorous and accurate because they do not consider the spectral mixture of different materials in the same pixel (Bannari *et al.*, 2003). The overall error, composed of errors in location of the sampling points in the validation sites (GPS), location of the sampling points in the IKONOS imagery and the image-to-image (hyperspectral) registration, leads to an uncertainty in the percentage residue cover retrieved from the Probe-1 imagery at the sampling points. An additional error is related to what the sensor actually “senses”. At off-nadir viewing angles, the sensor views a larger portion of the scene, which has an impact on the spectral signature and, subsequently, on the estimation of percent ground covers (White *et al.*, 2002). For Probe-1 with a 60° FOV, this resulted in an overestimation of the percent crop cover compared to the ground cover photos taken at nadir. In order to minimize these errors and to increase the accuracy of crop residue estimation using hyperspectral residue indices, image data must be acquired at the beginning or at the end of the agricultural season (Bannari *et al.*, 2006). In this period before significant crop growth, primarily only bare soil and residues are present. In this case, the estimation of percent residue cover can be drastically improved using hyperspectral data and other advanced methods as spectral mixture analysis (Bannari *et al.*, 2007b).

4. CONCLUSIONS

This study tested the performance of nine different hyperspectral crop residue indices (BI, CAI, NDI-1, NDI-2, SACRI-1, SACRI-2, MSACRI-1, MSACRI-2, and CRIM) on agricultural fields using two different and independent sources of data: ground-based reflectance measurements and hyperspectral Probe-1 data. The spectroradiometric ground-measurements were collected with a GER 3700 spectroradiometer over corn residues at various coverage rates. They

were convolved and resampled to the Probe-1 spectral band characteristics. The accuracy of these indices was examined using ground reflectance measurements obtained from vertical photographs.

The results indicated that, from the spectroradiometric ground-measurements, the CRIM and the MSACRI-1 are better for residue cover estimation, because they both take into account the soil line. From hyperspectral Probe-1 data, the MSACRI-1 showed the best results. However, in spite of this relative accuracy of this index, the percentage of crop residue estimation using hyperspectral crop residue indices is not entirely satisfactory. Indeed, all the considered indices suffer from saturation and linearity problems, and most of them are inaccurate to describe bare soil with no residue cover, except the MSACRI-1. Furthermore, in order to increase the performance of the approach as discussed in this paper, errors associated with locating the ground sampling points in the imagery, viewing the scene at off-nadir angles (Probe-1), shadow and classifying the ground photos must be further reduced. Acquisition of imagery during the post-harvest period or prior to spring seeding would simplify the extraction of percent residue cover by eliminating confusion with the crop canopy. Finally, the concept of the all the considered crop residue indices does not consider the spectral mixture of different materials in the same pixel. Certainly, other approaches such as unmixing or artificial neutral networks would allow improved discrimination between crop residue, bare soil and green crop cover.

ACKNOWLEDGMENTS

The authors would like to thank the Natural Sciences and Engineering Research Council (NSERC) and the University of Ottawa for financial support, and the Canada Centre for Remote Sensing (CCRS) for making the hyperspectral Probe-1 data available. We are grateful for the support and assistance of Jean-Claude Deguise (Agriculture and Agri-Food Canada in Ottawa, Ontario); Yann Pelcat (Indian Head Agricultural Research Foundation, Regina, Saskatchewan); Anne Smith and Karen Samuel (Agriculture and Agri-Food Canada in Lethbridge, Alberta). We would also like to thank the anonymous reviewers for their constructive comments.

REFERENCES

Aase, J.K., and Tanaka, D.L. (1991) Reflectance from four wheat residue cover densities as influenced by three soil backgrounds. Agronomy Journal, vol. 83, p. 753-757.

Arsenault, É. and Bonn, F. (2001) Evaluation of Soil Erosion Protective Cover by Crop Residues Using Vegetation Indices and Spectral Mixture Analysis of Multispectral and Hyperspectral Data. P. 299-308, *in* Duguay, C.R. et Bernier, M. (ed.) Proceedings of the 23rd Canadian Symposium on Remote Sensing. 21-24 August 2001, Canadian Aeronautics and Space Institute, Ottawa (Ontario), 900 p.

Bannari, A., Huete, A.R., Morin, D. and Bonn, F. (1995a) A Review of Vegetation Indices. Remote Sensing Reviews, vol. 13, p. 95-120.

Bannari, A., Morin, D., Bénié, G.B. and Bonn, F. (1995b) A Theoretical Review of Different Mathematical Models of Geometric Corrections Applied to Remote Sensing Images. Remote Sensing Reviews, vol. 13, p. 27-47.

Bannari, A., Huete, A.R., Morin, D. et Zagolski, F. (1996) Effets de la couleur et de la brillance du sol sur les indices de végétation. International Journal of Remote Sensing, vol. 17, n° 10, p. 1885-1906.

Bannari, A., Gibson, J.R. and Morin, D. (1997) The Necessity of Exterior Orientation Parameters for the Rigorous Geometric Correction of MEIS-II Airborne Digital Image. Remote Sensing Reviews, vol. 16, p. 135-156.

Bannari, A., Haboudane, D. et Bonn, F. (1999) Potentiel des mesures multispectrales pour la distinction entre les résidus de cultures et les sols nus sous-jacents. P. 359-366, *in* ERIM (ed.) Fourth International Airborne Remote Sensing Conference and Exhibition/21st Canadian Symposium on Remote Sensing, Ottawa, Ontario, Canada, 21-24 June 1999, vol. II, ERIM International Inc., Ann Arbor (Michigan), 907 p.

Bannari, A., Haboudane, D., et Bonn, F. (2000) Intérêt du moyen infrarouge pour la cartographie des résidus de cultures. Canadian Journal of Remote Sensing, vol. 26, n° 5, p. 384-393.

Bannari, A., Chevrier, M., Deguise, J.-C., McNairn, H. and Staenz, K. (2003) Senescent Vegetation Mapping Using Artificial Neutral Networks and Hyperspectral Remote Sensing. Vol. 7, p. 4292-4294, *in* IEEE-03CH37477 (ed.) International Geoscience and Remote Sensing Symposium (IGARSS'2003), Toulouse, France, 21-25 July 2003. InControl Production Inc., Monterey (California), 4630 p.

Bannari, A., Pacheco, A., Staenz, K., McNairn, H. and Omari, K. (2006) Estimating and Mapping Crop Residue Cover in Agricultural Lands Using Hyperspectral and IKONOS images. Remote Sensing of Environment, vol. 104, issue 4, p. 447-459.

Bannari, A., Khurshid, S.K., Staenz, K. and Schwarz, J. (2007a) A Comparison of Hyperspectral Chlorophyll Indices for Wheat Crop Chlorophyll Content Estimation Using Laboratory Reflectance Measurements. IEEE Transactions on Geosciences and Remote Sensing. (Under press)

Bannari, A., Staenz, K. and Khurshid, K.S. (2007b) Remote Sensing of Crop Residue Using Hyperspectral Hyperion (EO-1) Imagery. International Geoscience and Remote Sensing Symposium (IGARSS 2007), 23-27 July 2007, Barcelona (Spain), Proceedings on CD, 4 p.

Baret, F., Guyot, G. and Major, D.J. (1989) TSAVI: A vegetation index which minimizes soil brightness effets on LAI and APAR estimation. Vol. 3, p. 1355-1358, *in* IEEE (ed.) Proceedings of the IEEE International Geoscience and Remote Sensing Symposium

(IGARSS'89) and 12th Canadian Symposium on Remote Sensing, 10–14 July 1989, Vancouver, B.C., Canada, IEEE publication no 89CH2768-0, Piscataway (New Jersey), 3001 p.

Berk, A., Anderson, G.P., Acharya, P.K., Chetwynd, J.H., Bernstein, L.S., Shettle, E.P., Matthew, M.W. and Adler-Golden, S.M. (1999) MODTRAN 4 User's Manual. Air Force Research Laboratory, Hanscom AFB (Maryland), 99 p.

Biard, F., Bannari, A. et Bonn, F. (1995) SACRI (Soil Adjusted Corn Residue Index): un indice utilisant le proche et le moyen infrarouge pour la détection de résidus de cultures de maïs. P. 413-419, *in* Epp, H. and Taylor, C. (réd.) 17e Symposium canadien sur la télédétection, Saskatoon (Saskatchewan), 13 – 15 June 1995, Institut aéronautique et spatial du Canada, Ottawa (Ontario), 816 p.

Biard, F., and Baret, F. (1997) Crop Residue Estimation Using Multiband Reflectance. Remote Sensing Environment, vol. 59, p. 530-536.

Champagne, C., Staenz, K., Bannari, A., Deguise, J.-C., McNairn, H., and Shang, S. (2003) Validation of a Hyperspectral Curve-Fitting Model for the Estimation of Plant Water Content of Agricultural Canopies. Remote Sensing of Environment, vol. 87, p. 148-160.

Chevrier, M., Bannari, A., Deguise, J.-C., McNairn, H., and Staenz, K. (2002) Hyperspectal Narrow-Wavebands for Discriminating Crop Residue from Bare Soil. P. 2202-2204, *in* IEEE (ed.) IEEE International Geoscience and Remote Sensing Symposium (IGARSS'02) /24th Canadian Symposium on Remote Sensing, Toronto, Ontario, Canada, 24-28 June 2002, InControl Production Inc., Publication no 02CH37380, Monterey (California), 3114 p.

Chevrier, M. (2002) Potentiel de la télédétection hyperspectrale pour la cartographie des résidus de cultures. Mémoire de maîtrise, Département de géographie, Université d'Ottawa, Ottawa (Ontario), 170 p.

Cyr, L., Bonn, F., and Pesant, A. (1995) Vegetation indices derived from remote sensing for estimation of soil protection against water erosion. Ecological Modelling, vol. 79, no 3, p. 277-285.

Daughtry, C.S.T. (2001) Discriminating Crop Residues from Soil by Shortwave Infrared Reflectance. Agronomy Journal, vol. 93, no 1, p. 125-131.

Daughtry, C.S.T, McMurtrey, J.E., Chapelle, E.W., Hunter, W.J., and Steiner, J.L. (1996) Measuring Crop Residue Cover Using Remote Sensing Techniques. Theoretical and Applied Climatology, vol. 54, p. 17-26.

Daughtry, C.S.T., Hunt Jr., E.R. and McMurtrey, J.E. (2004) Assessing Crop Residues Cover Using Shortwave Infrared Reflectance. Remote Sensing of Environment, vol. 90, no 1, p. 126-143.

Daughtry, C.S.T., Hunt Jr., E.R., Doraiswamy, P.C. and McMurtrey, J.E. (2005) Remote Sensing the Spatial Distribution of Crop Residues. Agronomy Journal, vol. 97, no 3, p. 864-871.

Daughtry, C.S.T., Doraiswamy, P.C., Hunt Jr., E.R., Stern, J.E., McMurtrey, J.E. and Prueger, J.H. (2006) Remote Sensing of Crop Residues Cover and Soil Tillage Intensity. Soil and Tillage Research, vol. 91, p. 101-108.

Earth Search Sciences Inc. (2001) About Probe-1. Kalispell (Montana), www.earthsearch.com/technology.

Freebairn, D.M. and Wockner, G.H. (1986) A Study of Soil Erosion on Vertisols of the Eastern Darling Downs, Queensland 1: Effects of Surface Conditions on Soil Movement Within Sontour Bay Catchments. Australian Journal of Soil Science, vol. 24, p. 135-158.

Gao, B.C. and Goetz, A.F.H. (1990). Column atmospheric water vapor and vegetation liquid water retrieval from airborne imaging spectrometer data. Journal of Geophysical Research, vol. 95, p. 3549-3564.

Geophysical and Environmental Research Corporation (1990) GER 3700 Spectroradiometer User's Manual, version 2.1. Poughkeepsie, New York, 55 p.

Green, R.O., Conel, J.E., Margolis, J.S., Brugge, C.J. and Hoover, G.L. (1991) An inversion algorithm for the retrieval of atmospheric and leaf water absorption from AVIRIS radiance with compensation for atmospheric scattering. P. 51-61, *in* R.O. Green (ed.) Proceedings of the Third Annual Airborne Visible/Infrared Imaging Spectrometer (AVIRIS) Workshop. 20-21 May 1991, Pasadena (California), Jet Propulsion Laboratory (JPL) Publication 91-28, 321 p.

Haboudane, D., Bonn, F., Biard, F., Bannari, A. and Cliche, P. (1997) Shortwave Infrared Contribution to the Detection of Crop Residues and Dry Vegetation Over Different Soil Backgrounds. Paper no 195, Proceedings of the Geomatics in the Era of Radarsat GER'97 Symposium/19th Canadian Symposium on Remote Sensing, 25-30 May 1997, Ottawa (Ontario), Canada. Natural Resources Canada, Ottawa (Ontario), Proceedings on CD-ROM.

Hartwig, R.O. and Laflen, J.M. (1978) A meterstick method for measuring crop residue cover. Journal of Soil and Water Conservation, vol. 33, no 2, p. 90-91.

Huete, A.R. (1988) A soil-adjusted vegetation index (SAVI). Remote Sensing of Environment, vol. 25, p. 295-309.

Karimi, Y., Prasher, S.O., McNairn, H., Bonnell, R.B., Dutilleul, P. and Goel, P.K. (2005a) Discriminant analysis of hyperspectral data for assessing water and nitrogen stresses in corn. Transactions of American Society of Agricultural and Biological Engineers, vol. 48, p. 805-813.

Karimi, Y., Prasher, S.O., McNairn, H., Bonnell, R.B., Dutilleul, P. and Goel, P.K. (2005b) Classification accuracy of discriminant analysis, artificial neural networks and decision trees for weed and nitrogen stress detection in corn. Transactions of American Society of Agricultural and Biological Engineers, vol. 48, p.1261-1268.

Ketcheson, J.W., and Stonehouse, D.P. (1983) Conservation tillage in Ontario. Journal of Soils and Water Conservation, vol. 38, p. 253-254.

Labsphere (2001) A Guide to Reflectance Coatings and Materials. North Sutton (New Hampshire), http://www.labsphere.com/tech_info/docs/Coating_&_Material_Guide.pdf.

Major, D.J., Larney, F.L., and Lindwall, C.W. (1990) Spectral reflectance characteristics of wheat residue. P. 603-607, *in* IEEE (ed) Proceedings of the International Geoscience and Remote Sensing Symposium (IGARSS'90), University of Maryland, Washington, D.C., 20-24 May 1990. IEEE Publication no 90CH2825-8, Piscataway (New Jersey), vol. 1, 2485 p.

McNairn, H., and Protz, R. (1993) Mapping Corn Residue Cover on Agricultural Fields in Oxford County, Ontario, Using Thematic Mapper. Canadian Journal of Remote Sensing, vol. 19, n° 2, p. 152-159.

Morrison, J.E. and Chichester, F.W. (1991) Still video image analysis of crop residues covers. Soil Science Society of America, vol. 34, p. 2469-2474.

Morrison, J.E., Huang, C., Lightle, D.T. and Daughtry, C.S.T. (1993) Residues Cover Measurement Techniques. Journal of Soil and Water Conservation, vol. 48, p. 479-483.

Morrison, J.E., Lemunyon, J. and Bogusch, H.C. (1995) Source of variation and performance of nine devices when measuring crop residues cover. Transaction of American Society of Agricultural Engineers, vol. 38, p. 521-529.

Nagler, P.L., Inoue, Y., Glenn, E.P., Russ, A.L. and Daughtry, C.S.T. (2003) Cellulose absorption index (CAI) to quantify mixed soil-plant litter scenes. Remote Sensing Environment, vol. 87, p. 310-325.

Pacheco, A., Bannari, A. and McNairn, H. (2001) LAI Measurements in Beans and Corn Canopies with Two Optical Instruments. P. 374-379, *in* ISPRS-CNES (réd.) 8e Symposium international sur les mesures physiques et signatures en télédétection, Aussois (France), 8-12 janvier 2001, CNES, Toulouse, (France), 758 p.

Pacheco, A., Bannari, A., Staenz, K, Deguise, J.-C. and McNairn, H. (2002) Validating LAI Using Hyperspectral Imagery Over Agricultural Canopies. P. 210-215, *in* J.A. Sobrino (ed.) International Symposium on Recent Advances in Quantitative Remote Sensing. Valencia (Spain), 16-20 September 2002, Publications de la Universitat de València, València (Spain), 984 p.

Pacheco, A., Bannari, A., Staenz, K., Deguise, J.-C. and McNairn, H. (2007) Deriving Percent Crop Cover Over Agriculture Canopies Using Hyperspectral Remote Sensing. Canadian Journal of Remote Sensing, Special issue for hyperspectral remote sensing. (Under press)

PCI Geomatics (2000) Using PCI Software. Richmond Hill (Ontario), 540 p.

Rice, C.W. (2002) Storing Carbon in Soil : Why and How ? Geotimes, January, p. 1-5.

Rouse, J.W., Hass, R.W., Schell, J.A., Deering, D.W. and Harlan, J.C. (1974). Monitoring the vernal advancement and retrogradation (greenwave effect) of natural vegetation. NASA/GSFCT (Goddard Space Flight Center) Type III Final report, Greenbelt (Maryland), 164 p.

Secker, J., Staenz, K., Gauthier, R.P., and Budkewitsch, P. (2001) Vicarious Calibration of Hyperspectral Sensors in Operational Environments. Remote Sensing of Environment, vol. 76, p. 81-92.

Staenz, K., and Williams, D.J. (1997) Retrieval of Surface Reflectance from Hyperspectral Data Using a Look-Up Table Approach. Canadian Journal of Remote Sensing, vol. 23, n° 4, p. 354-368.

Staenz, K., Szeredi, T. and Schwarz, J. (1998) ISDAS A system for processing and analyzing hyperspectral data. Canadian Journal of Remote Sensing, vol. 24, n° 2, p. 99-113.

Streck, N.A., Rundquist, D. and Connot, J. (2002) Estimating Residual Wheat Dry Matter from Remote Sensing Measurements. Photogrammetric Engineering and Remote Sensing, vol. 68, n° 11, p. 1193-1201.

White, H.P., Sun, L., Staenz, K., Fernades, R., and Champagne, C.M. (2002) Determining the Contribution of Shaded Elements of a Canopy to Remotely Sensed Hyperspectral Signatures. P. 159-166, *in* J.A. Sobrino (ed.) Proceedings of the 1st International Symposium on Recent Advances in Quantitative Remote Sensing. Valencia (Spain), 16-20 September 2002, Publications de la Universitat de València, València (Spain), 984 p.

Wischmeier, W.H. and Smith, D.D. (1978) Predicting rainfall erosion losses - A guide to conservation planning. U.S. Department of Agriculture, Washington D.C., Agriculture Handbook, n° 537, 58 p.